Ionosphere of Callisto from Galileo radio occultation observations

A. J. Kliore,[1] A. Anabtawi,[1] R. G. Herrera,[1] S. W. Asmar,[1] A. F. Nagy,[2]
D. P. Hinson,[3] and F. M. Flasar[4]

Received 6 March 2002; revised 6 May 2002; accepted 8 May 2002; published 27 November 2002.

[1] An ionosphere has been detected at Callisto by the Galileo spacecraft, using the radio occultation technique. There were four usable occultations by Callisto, providing eight observation opportunities, all equatorial and near the terminator (entry and exit observations). Detectable electron densities were obtained from six of the eight opportunities. It was found that a detectable ionosphere was only present at the observed location when the trailing hemisphere of Callisto, which is the one that is impacted by the corotating plasma of Jupiter's magnetosphere, was illuminated by the Sun. Two of these observations yielded well-defined electron density profiles, having peak densities of 15,300 and 17,400 cm^{-3} at altitudes of 27.2 and 47.6 km and topside plasma scale heights of 29.6 and 49.0 km. Four different methods, based on both photoionization and electron impact ionization, were used to obtain estimates of the corresponding neutral densities at the surface. The various assumptions inherent in these methods required using a variety of parameters, (cross sections, rate constants, etc.) all with their associated uncertainties. It was rather surprising and reassuring to find that all of the methods used to estimate the surface neutral density gave very similar results in each of the eight cases. The estimated values fall between 1 and 3×10^{10} cm^{-3}, leading to an estimate for the column density of from 3 to 4×10^{16} cm^{-2}. *INDEX TERMS:* 6218 Planetology: Solar System Objects: Jovian satellites; 6028 Planetology: Comets and Small Bodies: Ionospheres—structure and dynamics; 6026 Planetology: Comets and Small Bodies: Ionospheres—composition and chemistry; 6025 Planetology: Comets and Small Bodies: Interactions with solar wind plasma and fields; *KEYWORDS:* Callisto, ionosphere, atmosphere, radio, occultation

Citation: Kliore, A. J., A. Anabtawi, R. G. Herrera, S. W. Asmar, A. F. Nagy, D. P. Hinson, and F. M. Flasar, Ionosphere of Callisto from Galileo radio occultation observations, *J. Geophys. Res.*, *107*(A11), 1407, doi:10.1029/2002JA009365, 2002.

1. Introduction

[2] The Galileo spacecraft, which was placed into orbit about Jupiter in December of 1995, has conducted a comprehensive tour of the Jovian system including multiple encounters of Io, Europa, Ganymede, and Callisto [*Johnson*, 2000]. Among the ten Galilean satellite encounters during the Galileo prime mission (Dec. 1995 to Dec. 1997) there were three radio occultations of the spacecraft by Europa, which produced the first observations of its ionosphere [*Kliore et al.*, 1997], and six distant radio occultations by Io, which defined the interaction of its ionosphere with Jupiter's magnetosphere [*Hinson et al.*, 1998]. During this phase of the mission, there was only one radio occultation by Callisto, which produced negative results. Fortunately, the prime mission was followed by the Galileo Europa Mission (GEM) lasting from Dec. 1997 to Dec. 1999, which provided three more radio occultations by Callisto (see Table 1). It is the data from these occultations that made possible the discovery of an ionosphere on Callisto and suggested an explanation for its apparently sporadic nature.

[3] The first observation of an atmosphere around Callisto was made from near infrared limb scans with the Galileo NIMS instrument, which indicated the presence of CO_2 up to a level of about 100 km, with a surface pressure of 7.5×10^{-9} mb and a temperature of 150 K [*Carlson*, 1999]. This is approximately equivalent to a surface density of CO_2 of about 3.6×10^8 cm^{-3}. Later, the Galileo RPWS instrument obtained an in situ measurement of a plasma density of 400 cm^{-3} at an altitude of about 535 km during the C22 flyby [*Gurnett et al.*, 2000], which was interpreted by the authors as indicating the presence of an ionospheric plasma around Callisto.

[4] This paper describes the unequivocal discovery, by means of Galileo radio occultation measurements, of a "classical" ionospheric layer having a peak above the surface and an approximately constant topside scale height.

[1]Jet Propulsion Laboratory, California Institute of Technology, Pasadena, California, USA.
[2]Space Physics Research Laboratory, University of Michigan, Ann Arbor, Michigan, USA.
[3]Center for Radar Astronomy, Stanford University, Stanford, California, USA.
[4]Laboratory for Extraterrestrial Physics, NASA Goddard Space Flight Center, Greenbelt, Maryland, USA.

0148-0227/02/2002JA009365

Table 1. Galileo Radio Science Measurements of the Ionosphere of Callisto

Observation	Date	Lat. deg	SZA deg	Ram deg	Psi deg	Detection
C9 N	6/25/99	2.2	81.5	105.7	172.9	none
C9 X	″	2.8	98.5	74.4	″	none
C20 N	**5/5/99**	**8.6**	**85.0**	**82.8**	**2.4**	**weak +**
C20 X	″	**0.8**	**101.3**	**99.2**	″	**weak +**
C22 N	**8/14/99**	**3.6**	**78.7**	**80.9**	**2.1**	**strong ++**
C22 X	″	**7.5**	**95.0**	**97.8**	″	**weak +**
C23 N	**9/16/99**	**6.6**	**82.5**	**81.7**	**1.0**	**strong ++**
C23 X	″	**3.6**	**97.6**	**98.9**	″	**weak +**

These measurements are summarized in Table 1, and a representation of the Callisto flyby trajectories is shown in Figure 1.

[5] In Table 1, the ram angle is defined as the angle between the magnetospheric ram direction (270°W. lon., 0° lat.) and the occultation tangency point, and Psi is the angle between the subsolar longitude and the ram direction (see Figure 3). From Figure 1 and Table 1, it is immediately obvious that flybys C20, C22, and C23 are practically identical, flying through the wake while the ram side is fully illuminated by the Sun. This was the result of using these flybys to lower Galileo's periapsis for subsequent close flybys of Io. In contrast, the C9 flyby occurs on the ram side while the opposite side of Callisto is fully illuminated. This difference will be seen to have a profound effect on the interpretation of the observations.

[6] The C30 flyby had a different geometry, in which the spacecraft's velocity vector was closely aligned with the direction to Earth. For this reason, and also because of the proximity to solar conjunction, no useful data were obtained from the C30 occultation.

2. Data and Processing

[7] The data used in producing these results were obtained by recording the S-band (2.3 GHz) signal from the Galileo spacecraft immediately before and after its occultation by Callisto. These data were taken at DSS 14 (Goldstone, CA) for C9, C20, and C22, and DSS 43 (Canberra, Australia) for C9 and C23, and were transmitted to Radio Science Operations at JPL, from where the data acquisition was controlled.

[8] They consisted of digitized samples (5,000 s^{-1}) of the signal in a 2,500 Hz passband which was "steered" by a programmable local oscillator (POCA) in an open-loop

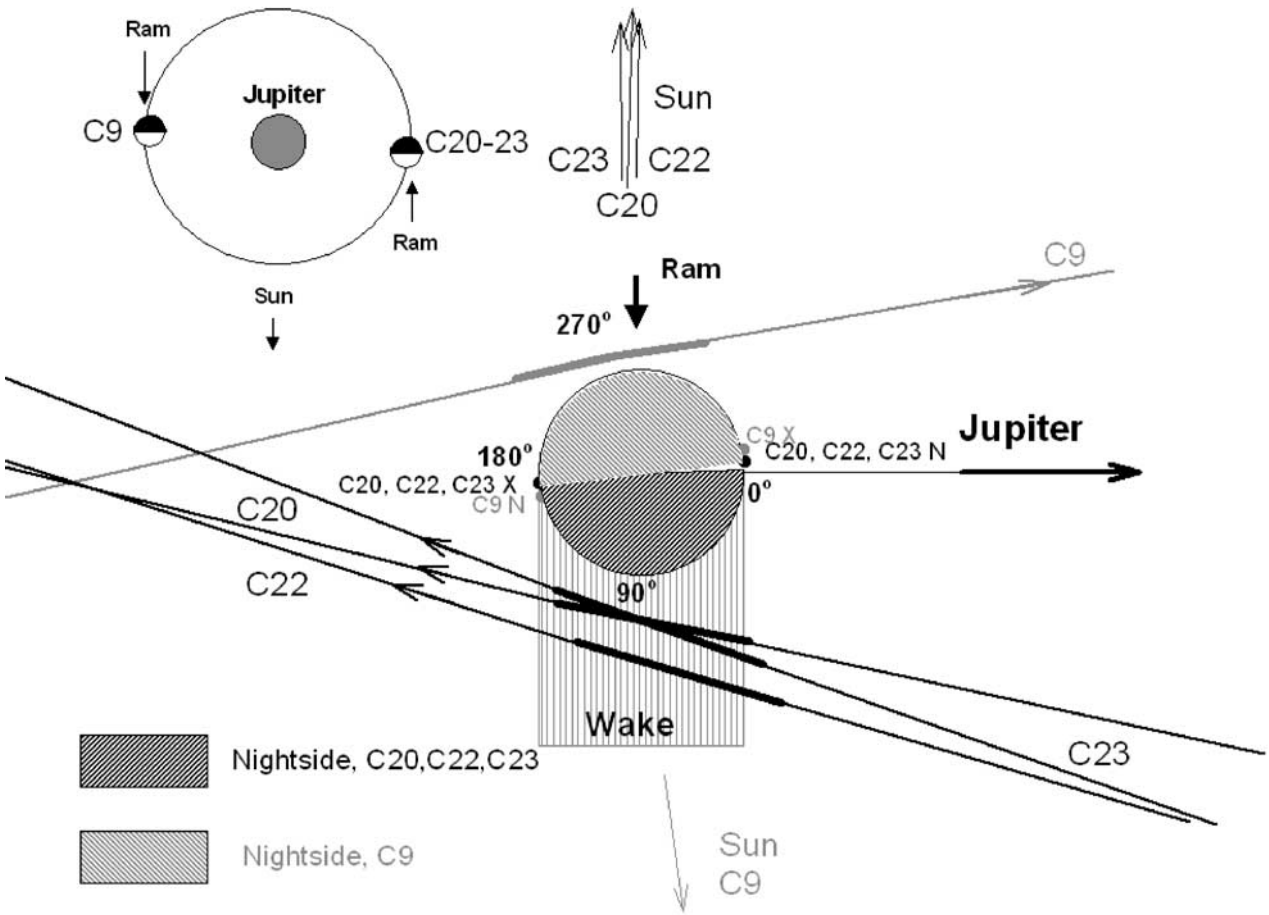

Figure 1. Callisto flyby geometry for the Galileo radio occultations, relative to the ram-wake axis (vertical). The direction to Jupiter has been chosen to always be to the right. (The approximate locations of the flybys on Callisto's orbit about Jupiter in relation to the direction of the Sun are shown in the inset).

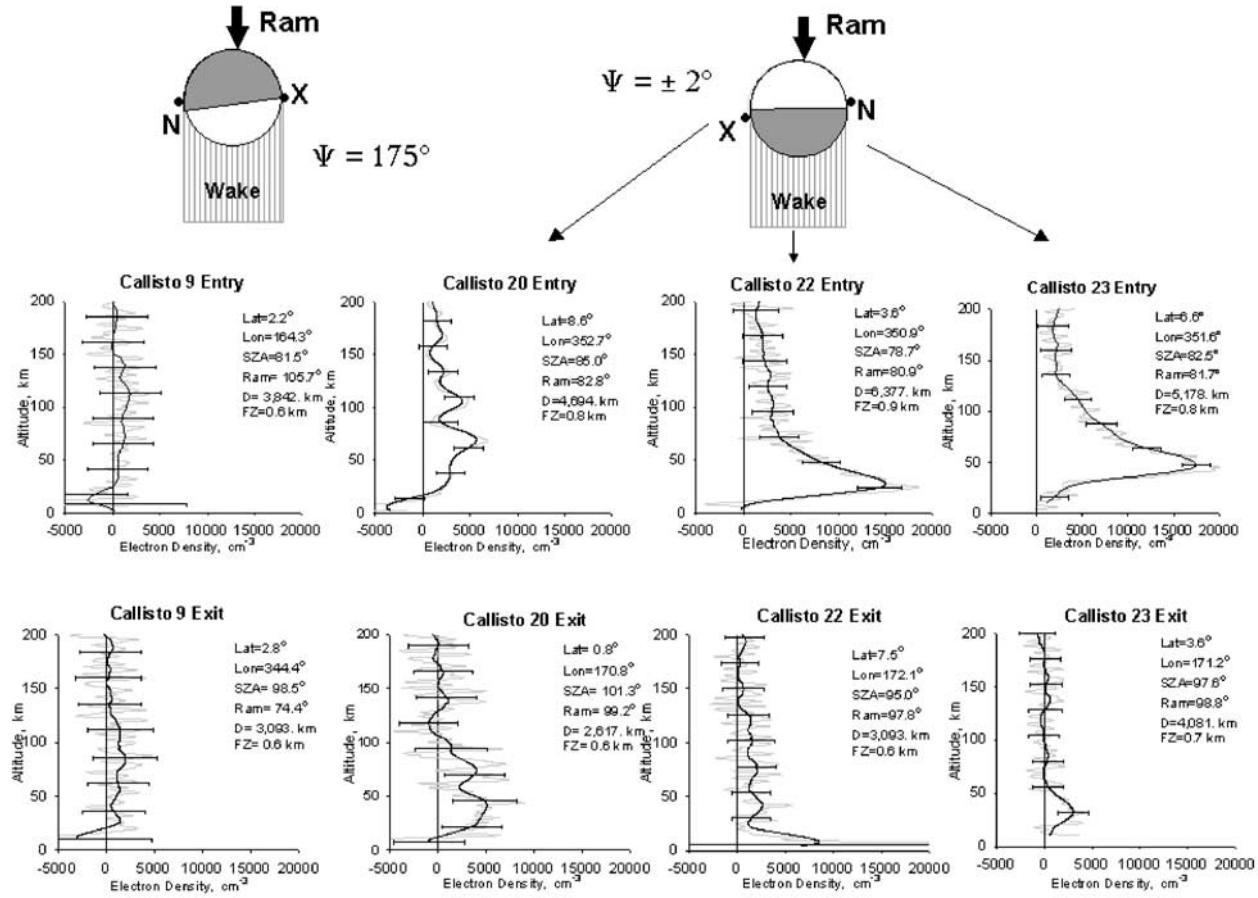

Figure 2. Electron density profiles derived from Galileo radio occultation observations of the Callisto ionosphere. The smoothed profiles are shown in black, and the unsmoothed ones in gray.

receiver to remove predicted frequency excursions due to the orbit of the spacecraft [*Herrera*, 1997; *Hinson et al.*, 1998; *Howard et al.*, 1992; *Kliore et al.*, 1997]. The digital data were then processed by the RSVP (Radio Science Validation and Data Processing) software maintained by the Radio Science Systems Group at JPL. This software employs a digital second-order phase-locked loop (PLL) to produce a time series of frequency and amplitude of the signal within the bandwidth of the open-loop receiver. The POCA function is then added back in to obtain the actual "sky frequency," and the Doppler frequency computed from the spacecraft trajectory is subtracted to obtain the frequency residuals, which contain the effects of propagation through the plasma environment of Callisto, and form the basic data of the radio occultation method. Each data set was typically processed through the PLL software three times, once with a loop time constant (ltc) of 1 s and a sampling interval of 1 s, and also with an ltc of 3 s, for sampling intervals of 0.1 s and 0.2 s. This was done to minimize any possible systematic effect either of the ltc or of the sampling interval upon the results.

3. Data Analysis and Results

[9] The data were analyzed using the method of integral inversion [*Fjeldbo and Eshleman*, 1968; *Kliore*, 1972] to obtain a vertical profile of the refractivity from the refractive bending angle determined by the Doppler residuals and the ephemeris of the spacecraft relative to Callisto. The refractivity is defined as:

$$N = (n - 1) \times 10^6 \tag{1}$$

where n is the refractive index, and it is then converted to electron density by:

$$n_e = -N \times f^2 / 4.034 \times 10^{13} \tag{2}$$

where n_e is the electron density (cm^{-3}) and f is the frequency (Hz). To provide some benchmark of what is being measured, a value of n_e of 1000 cm^{-3}, which is approximately the uncertainty in electron density results, corresponds to a refractivity of about 0.008.

[10] For each observation, electron density profiles were derived for four cases: one each from the data sets described in the previous section, and an additional one derived from the 0.1 s data set smoothed with a 5 point Lagrangian formula. These were linearly interpolated at 2 km intervals from 0 to 400 km altitude, and then averaged to form the final electron density profile for that observation. The error bars for each point were computed as follows:

$$\sigma_i = (\sigma_{i1} + \sigma_{i2})^{1/2} \tag{3}$$

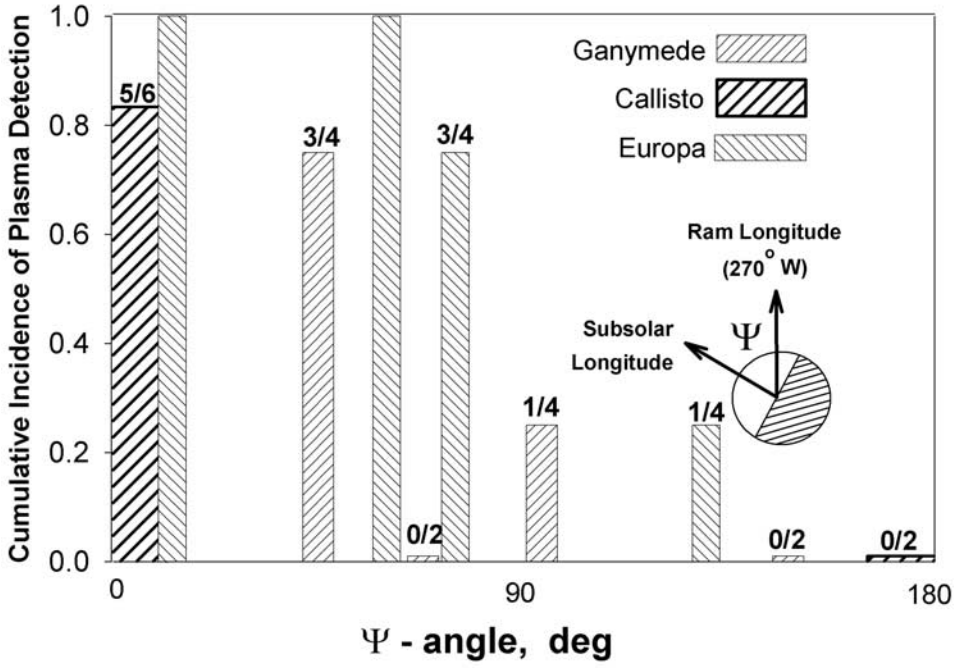

Figure 3. Cumulative incidence of detection as a function of the angle Ψ (see text). Results from Europa and Ganymede have been included to illustrate the dependence of the incidence of detection upon the angle Ψ.

where

$$\sigma_{i1}^2 = \frac{1}{4}\left(\sigma_{iA}^2 + \sigma_{iB}^2 + \sigma_{iC}^2 + \sigma_{iD}^2\right) \quad (4)$$

and A,B,C, and D denote the standard deviation of the mean of the baseline data for each of the four derivations, and σ_{i2} is the standard deviation of the average of the four data sets.

[11] The results from all eight usable observations are shown in Figure 2. The raw averaged electron density profiles are shown in gray. A 5% kernel smoothing transform [*SPSS*, 2000] was applied to obtain the smoothed profiles shown in black. With the exception of the C9 results, all of the profiles show evidence of the presence of an ionosphere. In Table 1, each measurement has been characterized as representing either a Strong Detection, a Weak Detection, or No Detection. No Detection (C9 Entry, C9 Exit) means that the measured electron density never exceeds the error bar. A Weak Detection (C20 Entry, C20 Exit, C22 Exit, and C23 Exit) is one in which the electron density does exceed the error bar, but the profile is not sufficiently smooth to determine a scale height. Finally, a Strong Detection (C22 Entry and C23 Entry) is one in which the electron density significantly exceeds the error bar, and the topside profile can be used to obtain a good estimate of the plasma scale height.

[12] The absence of any detectable ionosphere in the C9 measurements and the presence of at least a weakly detectable one in all of the C20, C22, and C23 measurements provides an important clue to the basic nature of the ionospheres of the Galilean satellites. Since all radio occultations in the Jovian system occur near the terminator, the only difference between any two measurements is the position of Callisto in its orbit at the time of the observation.

[13] This can be seen with reference to the inset diagram in Figure 1. The measurements of C9 were taken when the corotating plasma of Jupiter's magnetosphere was impinging on the dark hemisphere of Callisto, and those of C20, C22, and C23 all occurred about 180° away in Callisto's orbit, when the corotating plasma was impinging directly upon its sunlit hemisphere.

[14] This can also be seen in Figure 3, showing the cumulative incidence of detection as a function of the angle Ψ, which is the difference between the longitude of the center of the trailing hemisphere, where the impingement of the corotating magnetospheric particles is maximal (270° West), and the subsolar longitude. This angle varies between 0° and 180° as Callisto orbits Jupiter. The cumulative incidence of detection is simply a measure of success in detecting an ionosphere, and it is computed as the ratio of total detection points in a certain range of Ψ to the maximum possible. Two points are given for a "Strong Detection", one point for a "Weak Detection", and no points for "No Detection". Results for Europa and Ganymede are also presented further clarify the relationship between the incidence of detection and Ψ. Thus, in Figure 3 the average cumulative incidence is 0.722 for $0° < \Psi < 90°$, and 0.125 for $90° < \Psi < 180°$.

[15] These observations strongly suggest that an ionosphere observable by radio occultation exists on Callisto only when the trailing hemisphere is illuminated by the Sun. It should be pointed out that the Galileo plasma wave instrument detection of an "ionospheric-like" plasma in the vicinity of Callisto [*Gurnett et al.*, 2000] also took place

Table 2. Measured Ionospheric Properties and Inferred Atmospheric Densities for Callisto

Observation	SZA (deg)	Peak Altitude (km)	Peak Electron Density (cm^{-3})	Neutral Scale Height (km)	Inferred O_2 Density at the Surface (cm^{-3})	Inferred O_2 Column Density (cm^{-2})
C20 N	85.0	72.0	4,300 ± 4,40	–	–	–
C20 X	99.2	42.0	5,100 ± 3,300	–	–	–
C22 N	78.7	27.2 ± 1.5	15,300 ± 2,300	14.8 ± 0.2	PI - $2.14 \times 10^{10} \pm 1.28 \times 10^{10}$ EI - $1.76 \times 10^{10} \pm 2.73 \times 10^{9}$ C - $1.89 \times 10^{10} \pm 4.59 \times 10^{9}$	C - $2.80 \times 10^{16} \pm 6.81 \times 10^{15}$
C22 X	95.0	8.0	8,500 ± 17,000	–	–	–
C23 N	82.5	47.6 ± 1.5	17,400 ± 1,500	24.5 ± 0.9	PI - $1.89 \times 10^{10} \pm 2.00 \times 10^{8}$ EI - $1.49 \times 10^{10} \pm 2.81 \times 10^{9}$ C - $1.64 \times 10^{10} \pm 1.70 \times 10^{9}$	C-$4.01 \times 10^{16} \pm 4.40 \times 10^{15}$
C23 X	97.6	32.0	3,000 ± 1,600	–	–	–
				PI-Photoionization	EI-Electron Impact	C-Combined

during the C22 flyby, when this geometry existed and a "Strong Detection" was observed.

4. Discussion

[16] A summary of all positive observations is shown in Table 2. In the two instances where the electron density profiles are sufficiently distinct (C22N and C23N, where N stand for entry), the electron density scale height, H_e, is determined by fitting a straight line to the natural logarithm of the electron density on the topside, and determining its slope, as follows:

$$H_e = -1/\left[\frac{\partial}{\partial z}\{\ln n_e(z)\}\right] \tag{5}$$

[17] If the topside region is in chemical equilibrium, and the optical depth is small, then H_e is twice the neutral scale height, H_n [*Schunk and Nagy*, 2000].

[18] There are a number of different assumptions and approximations that can be used to obtain an estimate of the neutral gas density from which the observed ionosphere is produced. First, by analogy with Europa, it is reasonable to assume that the neutral atmosphere consists primarily of O_2 formed from dissociation of H_2O sputtered from Callisto's surface [*Hall et al.*, 1995; *Johnson et al.*, 1998].

[19] This assumption is not very restrictive, as the EUV photoabsorption cross sections of other possible atmospheric constituents, such as H_2O, O, H_2, OH, and H are similar to that of O_2.

[20] The next step is to assume that the observed electron density peaks are produced where the effective optical depth is unity, or:

$$n_n(z_p)H_n\sigma/\cos\chi = 1 \tag{6}$$

where $n_n(z_p)$ is the neutral density at the altitude of the peak, z_p, σ is the absorption cross section, H_n is the neutral scale height, and χ is the solar zenith angle. The neutral density at the peak is then:

$$n_n(z_p) = \cos\chi/H_n\sigma \tag{7}$$

[21] Finally, if we assume that the neutral density follows a diffusive equilibrium distribution to the surface, with a constant scale height, the density at the surface is:

$$n_n[z=0] = n_n(z_p)\exp(z_p/H_n) \tag{8}$$

[22] Using these assumptions and adopting a value of 2×10^{-17} cm^2 for the absorption cross section [*Schunk and Nagy*, 2000], leads to surface density values of $4.14 \times 10^{10} \pm 7.18 \times 10^{9}$ cm^{-3} and $1.87 \times 10^{10} \pm 5.12 \times 10^{9}$ cm^{-3} from the C22N and C23N profiles, respectively. These are plotted with filled black symbols and labeled $\tau = 1$ in Figure 4.

[23] There is another way to estimate the surface neutral density from the same electron density data, namely, by assuming that at the electron density peak the photoionization rate is equal to the recombination rate. This still assumes photochemical equilibrium, and that the peak is still where $\tau = 1$. This method is more sensitive to the assumption that the principal ion is O_2^+, because it requires a knowledge of the recombination rate (and thus the electron temperature).

[24] Starting out with the terrestrial solar maximum ionization frequency, ξ_E, (which gives a lower bound on the neutral density), the photoionization frequency at Jupiter can be obtained simply by taking into account the $1/r^2$ dependence. Thus the photoionization rate at Jupiter for $\tau = 1$, $P_J(z_p)$, can be written as:

$$P_J(z_p) = n_n(z_p)\xi_J[\tau=1] = n_n(z_p)\xi_E\{r_E/r_J\}^2\exp(-1) \tag{9}$$

[25] Taking $\xi_E = 1.59 \times 10^{-6}$ s^{-1} [*Schunk and Nagy*, 2000], leads to $\xi_J[\tau = 1] = 2.16 \times 10^{-8}$ s^{-1}. Equating the production rate to the loss rate, and assuming one major ion, which is lost via dissociative recombination, one gets:

$$n_n(z_p)\xi_J = n_e^2(z_p)\alpha \Rightarrow n_n(z_p) = n_e^2(z_p)\alpha/\xi_J \tag{10}$$

where α is the dissociative recombination constant. Taking α to have a value of 1.95×10^{-7} cm^3 s^{-1} (corresponding to an O_2^+ ionosphere with an electron temperature of 300 K), equations (10) and (8) yield inferred O_2 surface densities of $1.32 \times 10^{10} \pm 4.59 \times 10^{9}$ cm^{-3}, and $1.91 \times 10^{10} \pm 6.20 \times 10^{9}$ cm^{-3} for the data of C22N and C23N, respectively. These deduced densities are plotted with the filled black symbols and labeled P = L in Figure 4.

[26] The neutral density can also be estimated if electron impact ionization is assumed to produce the observed electron densities. It has been estimated that the energetic electron environment at Callisto consists of two "thermal" populations: one with a density of 0.02 cm^{-3} having a temperature of 2 keV, and the other 0.2–0.5 cm^{-3} with temperatures of 100 eV (J. Richardson, private communi-

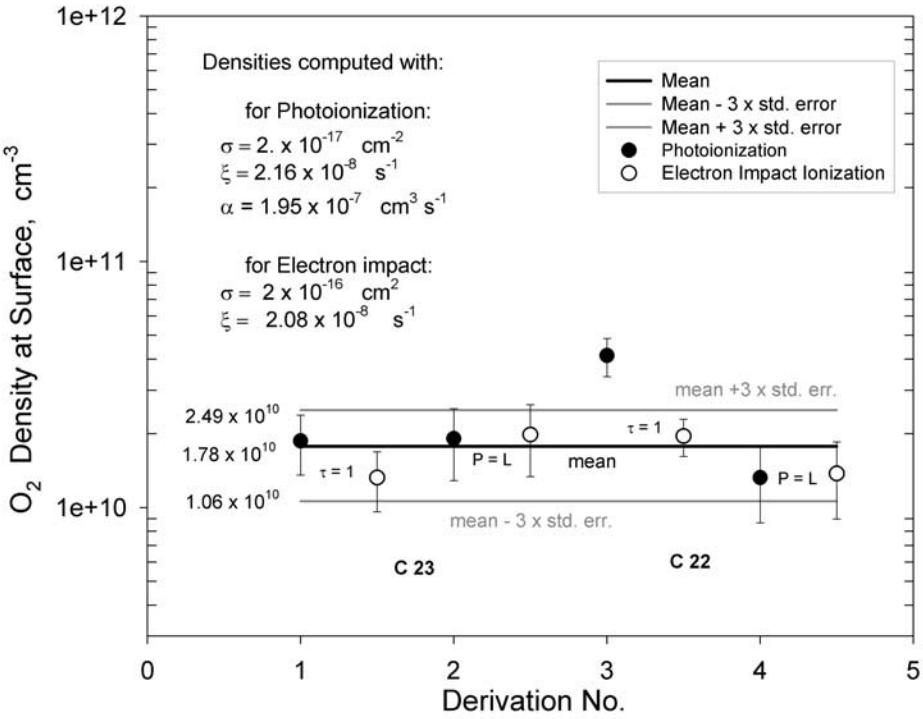

Figure 4. Estimates of the Callisto atmospheric density at the surface derived from the electron density profiles of C22N and C23N. The letters N designate an entry, or ingress, measurement.

cation, 2001). The corresponding ionization frequency ξ at $\tau = 1$ is then 2.08×10^{-8} s^{-1}, and a reasonable value for the absorption cross section is 2×10^{-16} cm^2 [*Banks and Kockarts*, 1979; *Rees*, 1989]. If the electron flux is assumed to be isotropic, cos χ in equation (7) is replaced by 1, and by applying it and equation (8) the density of O_2 at the surface computed from the data of C22N and C23N, is found to be $1.95 \times 10^{10} \pm 3.39 \times 10^9$ cm^{-3}, and $1.33 \times 10^{10} \pm 3.63 \times 10^9$ cm^{-3}, respectively. These values are plotted as open circles labeled $\tau = 1$ in Figure 4. Similarly, by equating production and loss, and using equation (10) with the new value of ξ, and equation (8), the inferred. O_2 surface densities from the C22N and C23N data were found to be $1.38 \times 10^{10} \pm 4.77 \times 10^9$ cm^{-3}, and $1.98 \times 10^{10} \pm 6.43 \times 10^9$ cm^{-3}, respectively. These values are plotted in Figure 4 as open circles labeled P = L.

[27] The average of the two derivations from the C22N observation using the photoionization assumptions yields an O_2 density at the surface of $2.14 \times 10^{10} \pm 1.28 \times 10^9$ cm^{-3}, and the data from C23N give a density of $1.89 \times 10^{10} \pm 2.00 \times 10^8$ cm^{-3}. These are listed in Table 2 with the prefix PI. The corresponding averages for the electron impact ionization assumptions are $1.76 \times 10^{10} \pm 2.73 \times 10^9$ cm^{-3} and $1.49 \times 10^{10} \pm 2.81 \times 10^9$ cm^{-3}, respectively, and they are listed in Table 2 with the prefix EI. When all four derivations for each data set are averaged, the resulting densities, marked with the prefix C in Table 2, are $1.89 \times 10^{10} \pm 4.59 \times 10^9$ cm^{-3} for C22N, and $1.64 \times 10^{10} \pm 1.70 \times 10^9$ cm^{-3} for C23N.

[28] In the final column of Table 2, the column density of O_2, calculated from the previously given surface densities and the respective scale heights, is tabulated for both data sets. The two results, prefixed by C, are quite similar, giving a value of $3–4 \times 10^{16}$ cm^{-2}.

[29] Finally, when all eight of the derived surface density values are averaged with weights corresponding to the reciprocal of the square of the normalized uncertainty, a density of $1.78 \times 10^{10} \pm 2.39 \times 10^9$ cm^{-3} is obtained. In Figure 4, this mean value is shown as the black horizontal line, and the gray lines indicate the limits of 3 times the standard error. From these results, it can be concluded that the inferred surface density of Callisto's O_2 atmosphere is between 1 and 3×10^{10} cm^{-3}.

5. Conclusions

[30] Here we presented electron density profiles obtained at Callisto by the Galileo spacecraft, using the radio occultation technique. There were five occultations by Callisto providing eight usable observation opportunities (entrance and exit observations). Detectable electron densities were obtained from six of the eight opportunities. It was found that the presence of a detectable ionosphere, at least in the equatorial terminator regions, coincided with solar illumination of the trailing hemisphere of Callisto.

[31] We estimated the corresponding neutral gas densities at the surface, considering photoionization, as well as electron impact ionization, as the source of the ionosphere. Furthermore, we used two somewhat independent approaches to deduce the neutral density from the measured electron densities. The various methods required using a variety of different parameters (cross sections, rate constants, etc.), all with different associated uncertainties. It was rather interesting and reassuring to find that all of the

various methods of estimating the surface neutral gas density gave very similar results. We find that these estimated values of the neutral atmosphere surface density all fall between $1-3 \times 10^{10}$ cm^{-3}.

[32] The fact that detectable ionospheres were only observed when the ramside was in sunlight appears to indicate that both plasma impact and photoionization are needed. One may be tempted to conclude that the impact of energetic ions from the magnetosphere of Jupiter is needed to sputter water and other molecules from the surface to create a neutral atmosphere [cf. *Cooper et al.*, 2001; *Johnson and Leblanc*, 2001; *Johnson et al.*, 1998] to be accompanied by photoionization to create an ionosphere. However, we feel that it is dangerous to speculate much beyond the facts, namely that detectable ionospheres were only observed when the ramside was sunlit.

[33] **Acknowledgments.** The authors wish to acknowledge the support and professional competence of the Galileo project, especially to W. J. O'Neill, R. T. Mitchell, J. M. Erickson, and E. E. Theilig, who managed the project over its long tenure, to T.V. Johnson, the Project Scientist, to the Radio Science Systems group at JPL, an to H. T. Howard, the leader of the Radio Propagation Team. The research reported herein was performed at the Jet Propulsion Laboratory of the California institute of Technology and at the University of Michigan with support from NASA contracts and grants.

[34] Arthur Richmond thanks Donald A. Gurnett and Robert E. Johnson for their assistance in evaluating this paper.

References

Banks, P. M., and A. G. Kockarts, *Aeronomy*, Academic, San Diego, Calif., 1979.

Carlson, R. W., A tenuous carbon dioxide atmosphere on Callisto, *Science*, *283*(5403), 820–821, 1999.

Cooper, J. F., R. E. Johnson, B. H. Mauk, H. B. Garrett, and A. N. Gehrels, Energetic ion and electron irradiation of the Galilean satellites, *Icarus*, *149*, 133–159, 2001.

Fjeldbo, G., and V. R. Eshleman, The atmosphere of Mars analyzed by integral inversion of Mariner IV occultation data, *Planet. Space Sci.*, *16*, 1035–1059, 1968.

Gurnett, D. A., A. M. Persoon, W. S. Kurth, A. Roux, and S. J. Bolton, Plasma densities in the vicinity of Callisto from Galileo plasma wave observations, *Geophys. Res. Lett.*, *27*(13), 1867–1870, 2000.

Hall, D. T., D. F. Strobel, P. D. Feldman, M. A. McGrath, and H. A. Weaver, Detection of an oxygen atmosphere on Jupiter's moon Europa, *Nature*, *373*, 677–679, 1995.

Herrera, R. G., Final report: Galileo radio science support team, Jet Propul. Lab., Pasadena, Calif., 1997.

Hinson, D. P., A. J. Kliore, F. M. Flasar, J. D. Twicken, P. J. Schinder, and R. G. Herrera, Galileo radio occultation measurements of Io's ionosphere and plasma wake, *J. Geophys. Res.*, *103*(A12), 29,343–29,357, 1998.

Howard, H. T., et al., Galileo radio science investigations, *Space Sci. Rev.*, *60*, 565–590, 1992.

Johnson, R. E., and F. Leblanc, The physics and chemistry of sputtering by energetic plasma ions, *Astrophys. Space Sci.*, *277*(1–2), 259–269, 2001.

Johnson, R. E., R. M. Killen, J. J. H. Waite, and W. S. Lewis, Europa's surface composition and sputter-produced ionosphere, *Geophys. Res. Lett.*, *25*, 3257–3260, 1998.

Johnson, T. V., The Galileo mission to Jupiter and its moons, *Sci. Am.*, *282*(2), 40–49, 2000.

Kliore, A. J., Current methods of radio occultation data inversion, in *The Mathematics of Profile Inversion*, edited by L. Colin, pp. 3–2 to 3–17, NASA Ames Res. Cent., Moffett Field, Calif., 1972.

Kliore, A. J., D. P. Hinson, F. M. Flasar, A. F. Nagy, and T. E. Cravens, The Ionosphere of Europa from Galileo radio occultations, *Science*, *277*(5324), 355–357, 1997.

Rees, M. H., *Physics and Chemistry of the Upper Atmosphere*, Cambridge Univ. Press, New York, 1989.

Schunk, R. W., and A. F. Nagy, *Ionospheres*, Cambridge Univ. Press, New York, 2000.

SPSS, *SigmaPlot 2000 Programming Guide*, SPSS, Inc., Chicago, Ill., 2000.

A. Anabtawi, S. W. Asmar, R. G. Herrera, and A. J. Kliore, Jet Propulsion Laboratory, California Institute of Technology, 4800 Oak Grove Drive, Pasadena, CA 91109, USA. (akliore@jpl.nasa.gov)

F. M. Flasar, Laboratory for Extraterrestrial Physics, NASA Goddard Space Flight Center, Greenbelt, MD 20771, USA.

D. P. Hinson, Center for Radar Astronomy, Stanford University, Stanford, CA 94305-9515, USA.

A. F. Nagy, Space Physics Research Laboratory, University of Michigan, Ann Arbor, MI 48109-2143, USA.